

Construction of Larger Molecular Aluminophosphate Cages from the Cyclic Four-Ring Building Unit

Jan Chyba,^{†,‡} Zdenek Moravec,^{†,‡} Marek Necas,^{†,‡} Sanjay Mathur,[§] and Jiri Pinkas^{*,†,‡}

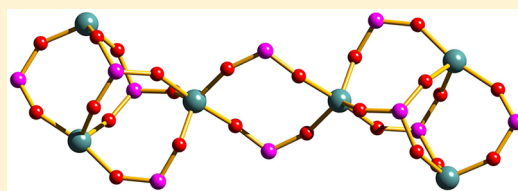
[†]Department of Chemistry, Faculty of Science, Masaryk University, Kotlarska 2, CZ-61137 Brno, Czech Republic

[‡]Central European Institute of Technology (CEITEC), Masaryk University, CZ-62500 Brno, Czech Republic

[§]Institute of Inorganic Chemistry, University of Cologne, Greinstrasse 6, D-50939, Cologne, Germany

Supporting Information

ABSTRACT: New molecular aluminophosphates of different nuclearity are synthesized by a stepwise process and structurally characterized. The alkane elimination reaction of bis(trimethylsiloxy)phosphoric acid, OP(OH)(OSiMe₃)₂, with trialkylalanes, AlR₃ (R = Me, Et, ^tBu), provides the cyclic dimeric aluminophosphates, [(AlR₂{μ₂-O₂P(OSiMe₃)₂})₂] (R = Me (1), Et (2), ^tBu (3)). Unsymmetrically substituted cyclic aluminophosphate [(AlMe₂{μ₂-O₂P(OSiMe₃)^c(Hex)})₂] (*cis/trans*-4) is prepared by dealkylsilylation reaction of ^cHexP(O)(OSiMe₃)₂ with AlMe₃. Molecules 1–4 containing the [Al₂(μ₂-O₂P)] inorganic core are structural and spectroscopic models for the single four-ring (S4R) secondary building units (SBU) of zeolite frameworks. Compound 1 serves as a starting point in construction of larger molecular units by reactions with OP(OH)(OSiMe₃)₂ as a cage-extending reagent and with diketones, such as Hhfacac (1,1,1,5,5,5-hexafluoropentan-2,4-dione) and Hacac (pentan-2,4-dione), as capping reagents. Reaction of 1 with 4 equiv of Hhfacac leads to new cyclic aluminophosphate [(Al(hfacac)₂{μ₂-O₂P(OSiMe₃)₂})₂] (5), existing in two isomeric (*D*₂ and *C*_{2h}) forms. Reaction of 1 with 2 equiv of OP(OH)(OSiMe₃)₂ and 1 equiv of Hhfacac provides a molecular aluminophosphate [AlMe{Al(hfacac)}₂{μ₃-O₃P(OSiMe₃)₂}{μ₂-O₂P(OSiMe₃)₂}{OP(OSiMe₃)₃}] (6), while by adding first the Hhfacac and using 3 equiv of OP(OH)(OSiMe₃)₂ we isolate [Al{Al(hfacac)}₂{μ₃-O₃P(OSiMe₃)₂}{μ₂-O₂P(OSiMe₃)₂}]H{OP(O)(OSiMe₃)₂} (7). These molecules contain units in their cores that imitate 4=1 SBU of zeolite frameworks. Reaction with the order of component mixing 1, Hhfacac, OP(OH)(OSiMe₃)₂ at a 1:2:2 molar ratio lead to formation of a larger cluster [(Al(AlMe){Al(hfacac)}₂{μ₃-O₃P(OSiMe₃)₂}{μ₂-O₂P(OSiMe₃)₂})₃] (8) containing both S4R and 4=1 structural units. Similarly, Hacac (pentan-2,4-dione) provides an isostructural [(Al(AlMe){Al(acac)}₂{μ₃-O₃P(OSiMe₃)₂}{μ₂-O₂P(OSiMe₃)₂})₃] (9). Both molecules display Al centers in three different coordination environments.



INTRODUCTION

Aluminophosphates constitute an important and extensive class of inorganic open-framework materials.¹ They form porous zeolite-like structures based on networks of alternating corner-sharing AlO_x (*x* = 4, 5, 6) polyhedra and PO₄ tetrahedra. The self-assembly process is influenced by the templating effect² in hydrothermal,³ solvothermal,⁴ or ionothermal⁵ synthetic reactions. Because of the presence of channels and pores of molecular dimensions, aluminophosphates have been used as adsorbents and catalysts.⁶ Isomorphous substitution of transition metals for Al and/or P in the framework⁷ led to catalysts possessing, besides the shape selectivity, Brønsted and Lewis acidity and redox functionality.^{8,9} The synthetic process is still mostly empirical, although some advances in the direction of rational design have been made.¹⁰ While the traditional four-connected AlPO₄ phases are usually prepared under hydrothermal conditions, low-dimensional, chain, and layer aluminophosphates with an Al/P ratio lower than 1 were synthesized in mostly nonaqueous solvents.^{11–13} Besides the classical view of assembly of molecular building units as the underlying mechanism of crystallization of porous solids,^{14–16} a new complementary model for formation of aluminophosphates based on stepwise transformations of a parent chain to

other linear structures, layers, and finally to open frameworks was proposed.¹⁷ The chains are built of corner- or edge-sharing [Al₂(μ₂-O₂PO₂)₂] single four rings (S4R), and their hydrolysis/condensation leads to cross-linking to the porous layers and subsequently to three-dimensional framework structures. In related work on open-framework zinc phosphates, a similar conclusion on the mechanism was formulated as it was shown that low-dimensional structures, such as small clusters, serve as the starting species that condense to chains or ladders and subsequently transform to layers to finally form 3D frameworks.^{18,19} This increasing tendency to rationalize the synthesis turned the focus of research on finding new bottom-up approaches to aluminophosphates. In an effort to contribute to elucidation of the crystallization mechanism, the synthesis and transformations of molecular aluminophosphate and -phosphate compounds soluble in organic solvents were studied as potential precursors and spectroscopic models for secondary building units (SBU, Chart 1S, Supporting Information).^{20,21} The simplest of them are S4R,^{22–28} and they also proved to be convenient single-source precursors for nonaqueous synthesis

Received: January 13, 2014

Published: March 11, 2014

of aluminophosphate materials.^{23,27} Other molecular structural units include complexes of various nuclearity and geometries of central inorganic cores, such as cubic D4R,^{20,22,28–32} hexagonal drum D6R,^{28,32,33} single six-ring S6R,³⁴ tricyclic 6=1,³⁵ bicyclic 4=1,^{36,37} or large octameric,³⁸ decameric,^{28,32,38,39} and dodecameric^{40,41} clusters.

Molecular aluminophosphates and -phosphonates have been predominantly synthesized by reactions of phosphonic acids or alkoxy and aryloxy esters of phosphoric acid with aluminum alkyls, alkoxides, or halides (for selected examples see Scheme 1

Scheme 1. Elimination Reactions Leading to S4R Aluminophosphates and Aluminophosphonates

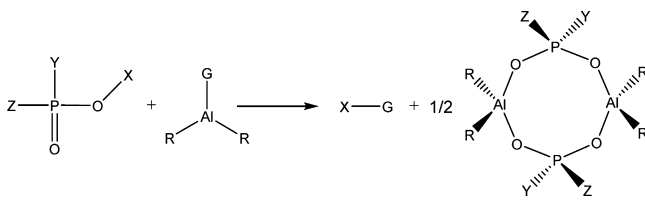


Table 1. Cyclic Aluminophosphates and Aluminophosphonates (S4R) Synthesized by Different Elimination Reactions According to Scheme 1

X	Y	Z	R	G	X–G	product
SiMe ₃	OSiMe ₃	OSiMe ₃	Me	Cl	Me ₃ SiCl	1 ²⁴
SiMe ₃	OSiMe ₃	OSiMe ₃	Et	Cl	Me ₃ SiCl	2 ²⁴
SiMe ₃	OSiMe ₃	OSiMe ₃	^t Bu	Cl	Me ₃ SiCl	10 ²²
SiMe ₃	OSiMe ₃	OSiMe ₃	Me	Me	Me ₄ Si	1 ²⁴
SiMe ₃	OSiMe ₃	OSiMe ₃	Et	Et	Me ₃ SiEt	2 ²⁴
SiMe ₃	OSiMe ₃	^c Hex	Me	Me	Me ₄ Si	4, this work
H	O ^t Bu	O ^t Bu	Me	Me	MeH	11 ²³
H	OSiMe ₃	^t Bu	Me	Me	MeH	12 ²⁵
H	OSiMe ₃	OSiMe ₃	Me	Me	MeH	1, this work
H	OSiMe ₃	OSiMe ₃	Et	Et	EtH	2, this work
H	OSiMe ₃	OSiMe ₃	^t Bu	^t Bu	^t BuH	3, this work
H	O ^{Ph}	O ^{Ph}	Me	Me	MeH	26
H	O ^{Ph}	O ^{Ph}	Et	Et	EtH	26
H	O ^{Ph}	O ^{Ph}	^t Bu	^t Bu	^t BuH	13 ²⁶
H	O ^t Bu	O ^t Bu	O ⁱ Pr	O ⁱ Pr	ⁱ PrOH	(14) ₂ ²³
H	OH ^a	Me	^t Bu	^t Bu	^t BuH	28

^aOH was subsequently silylated by Me₃SiNMe₂ to OSiMe₃.

and Table 1). These reactions are based on elimination of trimethylsilylchloride, alkanes, alkylsilanes, or alcohols. We are interested in developing reaction protocols leading to polyhedral aluminophosphates and -phosphonates and specifically in our novel synthetic route based on dealkylsilylation of trimethylsilylestere of phosphoric and phosphonic acids in the reaction with organoaluminum compounds.^{24,42,43} As the number of well-characterized molecular aluminophosphates and -phosphonates, which could serve as precursors and models of aluminophosphate structural units, is relatively limited, we decided to study the synthesis of new S4R molecules by alkane and alkylsilane elimination. Furthermore, we explored their subsequent transformations to larger entities with the Al/P ratio lower than 1 by employing OP(OH)(OSiMe₃)₂ as cage-extending reagent. We also applied reactions with Hhfacac and Hacac as capping agents that would modify the reactivity of

aluminum centers by forming chelates. Here we report our results on the synthesis of nine new molecular aluminophosphates and -phosphonates as well as their structural analyses and spectroscopic characterization.

EXPERIMENTAL SECTION

General Procedures. All manipulations were performed under a dry nitrogen atmosphere by Schlenk techniques or in a MBraun Unilab drybox maintained under 1 ppm of O₂ and H₂O. Solvents were dried over and distilled from Na/benzophenone under nitrogen. C₆D₆ and toluene-*d*₈ were dried over and distilled from Na/K alloy, while P₄O₁₀ was used for CDCl₃ and CD₂Cl₂. Solvents were degassed prior to use. AlMe₃, AlEt₃ (Sigma-Aldrich, 2 M in toluene), and Al^tBu₃ (Sigma-Aldrich, 1 M in hexane) were used as received. OP(OH)(OSiMe₃)₂ was prepared by a modified procedure from KH₂PO₄ and Me₃SiCl.⁴⁴ NMR spectra (¹H, ¹³C, ²⁷Al, ²⁹Si, and ³¹P) were acquired on Bruker AVANCE DRX 500 and 300 MHz spectrometers. Chemical shifts were referenced to the residual protic impurities or solvent resonances (¹H and ¹³C) or externally to Al(acac)₃, SiMe₄, and H₃PO₄ (²⁷Al, ²⁹Si, and ³¹P). Solid-state NMR spectra (¹³C, ²⁷Al, ²⁹Si, and ³¹P) were collected on a wide-bore Varian INOVA 400 NMR spectrometer (University of Tennessee) with a broad-band Chemagnetic 5 mm MAS probe. Inside a drybox, samples were loaded into 5 mm pencil rotors, stoppered with Teflon plugs, and sealed with silicon grease and paraffin wax. Magic angle spinning rates were 5 kHz for ²⁹Si and ¹³C CPMAS and 10 kHz for ²⁷Al and ³¹P MAS spectra. Chemical shifts were referenced externally to ³¹P δ [H₃PO₄ (85%)] 0.0 ppm, ²⁹Si δ [(Me₃SiO)₈Si₈O₂₆] 11.72 ppm, ²⁷Al δ [Al(H₂O)₆³⁺] 0.0 ppm, ¹³C δ [adamantane] 38.68 ppm. IR spectra (4000–400 cm⁻¹) were collected on Bruker EQUINOX 55/S/NIR and TENSOR 27 FTIR spectrometers. Samples were prepared as KBr pellets. CHN elemental analyses were carried out by Instituto de Química, UNAM. Melting points were measured in sealed capillaries and are uncorrected. Thermal analysis (TG/DSC) was measured on a Netzsch STA 449C Jupiter apparatus from 25 to 1100 °C under flowing air (70 mL min⁻¹) with a heating rate of 5 K min⁻¹. APCI-MS measurement was performed on an Agilent 6224 TOF LC-MS system. Solid samples were dissolved in toluene. Samples were injected via syringe pump KDS model 100 Series (KD Scientific, Inc., USA) into the electrospray ion source at a flow rate of 30 μL min⁻¹ for 2 min long analyses. Spectra were recorded both in positive and in negative mode for *m/z* 30–3200 Da at 4 GHz tuning for high-resolution instrument mode. A drying gas temperature of 200 °C and drying gas flow of 7 l/min with 30 psig for the nebulizer pressure were used for ionization of analytes in ion source/ESI. The fragmentor was set to 10 V, and the capillary voltage was –2000/4000 V (±APCI). Single-crystal diffraction data were collected on a KUMA KM-4 κ-axis diffractometer with graphite-monochromated Mo Kα radiation (λ = 0.71073 Å) and a CCD camera at 120 K. Intensity data were corrected for Lorentz and polarization effects. Details of data collection and refinement are summarized in Table 2. The structure was solved by direct methods and refined by full-matrix least-squares methods using the SHELXTL program package.⁴⁵ H atoms were positioned geometrically and refined as riding.

Synthesis of [(AlR₂{μ₂-O₂P(OSiMe₃)₂)}₂], R = Me (1), Et (2). A solution of OP(OH)(OSiMe₃)₂ (2.00 mmol, 484 mg) in toluene (2.0 mL) and a 2.0 M solution of AlR₃ (2.0 mmol, 1.0 mL) were simultaneously added to 5.0 mL of toluene at 0 °C. After mixing of components, an ice bath was removed and the reaction mixture stirred at room temperature until gas evolution ceased. All volatile components were removed under vacuum. Crystals were grown by slow cooling of a saturated hexane solution. Yields of 1 and 2 (80%) were comparable to previously published results, and crystal and spectroscopic data agree with the literature.²⁴

Synthesis of [(Al^tBu₂{μ₂-O₂P(OSiMe₃)₂)}₂] (3). A solution of OP(OH)(OSiMe₃)₂ (2.00 mmol, 484 mg) in hexane (2.0 mL) and a solution of Al^tBu₃ (1.0 M, in hexane, 2.0 mmol, 2.0 mL) were simultaneously added dropwise to hexane (5.0 mL) at 0 °C. The resulting mixture was stirred at room temperature for 2 days. All

Table 2. Crystallographic Data and Structure Refinement Parameters for Compounds 4 and 6–9

	4	6	7	8	9
empirical formula	C ₂₂ H ₅₂ Al ₂ O ₆ P ₂ Si ₂	C ₃₈ H ₈₆ Al ₃ F ₁₂ O ₂₄ P ₃ Si ₉	C ₄₀ H ₉₃ Al ₃ F ₁₂ O ₂₈ P ₆ Si ₁₀ · 1/8 C ₆ H ₁₄	C ₆₀ H ₁₅₂ Al ₆ F ₁₂ O ₄₄ P ₁₀ Si ₁₆ · 2THF	C ₆₀ H ₁₆₄ Al ₆ O ₄₄ P ₁₀ Si ₁₆
fw	584.72	1643.67	1808.58	2871.04	2510.93
cryst syst	triclinic	monoclinic	triclinic	triclinic	triclinic
space group	$P\bar{1}$	$P2_1/c$	$P\bar{1}$	$P\bar{1}$	$P\bar{1}$
temp., K	120(2)	120(2)	120(2)	120(2)	120(2)
λ , Å	0.71073	0.71073	0.71073	0.71073	0.71073
a , Å	8.5098(10)	17.207(2)	14.6903(2)	13.9324(3)	13.9640(4)
b , Å	10.6686(10)	21.720(3)	16.3775(2)	16.0191(4)	17.0083(8)
c , Å	10.8765(17)	21.770(3)	23.1011(4)	16.7797(5)	17.4120(7)
α , deg	98.789(14)	90	92.7310(10)	81.927(2)	61.565(3)
β , deg	112.477(12)	91.442(13)	107.4470(10)	77.855(2)	83.837(3)
γ , deg	107.401(9)	90	114.682(2)	77.631(2)	79.157(4)
V , Å ³	829.76(23)	8134(2)	4721.04(12)	3558.29(16)	3570.8(2)
Z	1	4	2	1	1
μ , mm ⁻¹	0.287	0.365	0.352	0.378	0.354
no. of reflns collected	6386	86 474	56 277	42 811	41 330
no. of indep reflns (R_{int})	2860 (0.0382)	14 302 (0.0185)	16 544 (0.0281)	12 482 (0.0386)	11 822 (0.0706)
no. of data/restraints/params	2860/0/154	14 302/108/908	16 544/928/1292	12 482/6/747	11 822/427/805
GoF on F^2	0.979	1.075	1.088	1.058	1.040
$R_1, \sigma wR_2^b$ ($I > 2\sigma(I)$)	0.0457, 0.1132	0.0448, 0.1228	0.0686, 0.2194	0.0539, 0.1439	0.0702, 0.2290
$R_1, \sigma wR_2^b$ (all data)	0.0803, 0.1227	0.0654, 0.1331	0.0990, 0.2317	0.0976, 0.1739	0.1050, 0.2409
largest diff. peak/hole, e ⁻ Å ⁻³	0.357/−0.282	1.106/−0.779	1.426/−0.622	0.709/−0.410	1.886/−0.723

$$^a R_1 = \sum |F_o| - |F_c| / \sum |F_o|, \quad ^b wR_2 = [\sum w(F_o^2 - F_c^2)^2 / \sum (F_o^2)^2]^{1/2}.$$

volatile components were removed under vacuum. Crystals grown at -25 °C from saturated hexane solution were unsuitable for X-ray diffraction analysis. Yield: 0.50 g (65%). Mp: 96–98 °C. ¹H NMR (300.1 MHz, CDCl₃): δ −0.18 (d, ³J_{HH} = 7.0 Hz, 8H, AlCH₂CH(CH₃)₂), 0.26 (s, 36H, POSi(CH₃)₃), 0.89 (d, ³J_{HH} = 6.6 Hz, 24H, AlCH₂CH(CH₃)₂), 1.81 (app-non, ³J_{HH} = 6.6 Hz, 4H, AlCH₂CH(CH₃)₂). ¹³C APT NMR (75.5 MHz, CDCl₃): δ 0.84 (d, ³J_{PC} = 2.1 Hz, POSi(CH₃)₃), 22.55 (br s, AlCH₂CH(CH₃)₂), 26.16 (s, AlCH₂CH(CH₃)₂), 28.49 (s, AlCH₂CH(CH₃)₂). ²⁹Si{¹H} NMR (59.6 MHz, CDCl₃): δ 22.9 (d, ²J_{PSi} = 5.1 Hz). ³¹P{¹H} NMR (121.5 MHz, CDCl₃): δ −29.6 (s). IR (KBr pellet, cm⁻¹): ν 2948 m, 2862 m, 2784 w, 1465 w, 1421 w, 1377 w, 1361 w, 1319 w, 1259 s (δ CH₃), 1223 s, 1180 m, 1129 s (ν PO), 1062 vs (ν SiO), 855 vs (ρ CH₃), 762 m (ρ CH₃), 680 m, 613 w. MS (EI 30 eV), m/z (rel int %): 702 (42) [M − tBu]⁺, 648 (100) [M − SiMe₃ − (CH₃)₂CH]⁺, 73 (90) [Si(CH₃)₃]⁺. Anal. Calcd for C₂₈H₇₂Al₂O₈P₂Si₄: C, 43.95; H, 9.49. Found: C, 42.94; H, 9.27.

Synthesis of [(AlMe₂(μ₂-O₂P(OSiMe₃)(Hex))₂]₂ (4). To a stirred solution of HexP(O)(OSiMe₃)₂ (2.06 mmol, 634 mg) in toluene (5 mL), a solution of AlMe₃ in toluene (2.0 M, 1.0 mL, 2.0 mmol) was added. The reaction mixture was heated under reflux at 120 °C for 3 days and then concentrated to 1 mL. Subsequent slow cooling to -25 °C provided colorless crystals suitable for X-ray diffraction analysis. Yield: 0.261 g (45%). Mp: 96–100 °C. ¹H NMR (300.1 MHz, CDCl₃): δ −1.18 (s, *cis*-Al(CH₃)₂), −1.16 (s, *trans*-Al(CH₃)₂), −1.15 (s, *cis*-Al(CH₃)₂), all three signals 12H, 0.06 (s, 18H, POSi(CH₃)₃), 1.00–1.71 (m, 22H, PC₆H₁₁). ¹³C APT NMR (75.5 MHz, CDCl₃): δ −9.57 (br s, AlCH₃), 1.07 (d, ³J_{PC} = 1.1 Hz, POSi(CH₃)₃), 1.12 (d, ³J_{PC} = 1.4 Hz, POSi(CH₃)₃), 26.03–26.42 (m, PCH(CH₂)₅), 36.63 (d, ¹J_{PC} = 156.0 Hz, PCH(CH₂)₅), 36.67 (d, ¹J_{PC} = 156.6 Hz, PCH(CH₂)₅). ²⁹Si{¹H} NMR (59.6 MHz, CDCl₃): δ 22.4 (s), 22.6 (s). ³¹P{¹H} NMR (121.5 MHz, CDCl₃): δ 12.7 (s, *cis*), 13.0 (s, *trans*). IR (KBr pellet, cm⁻¹): ν 2933 s, 2857 m, 1452 m, 1283 m, 1258 s (δ CH₃), 1219 s, 1204 vs, 1177 m, 1130 s, 1105 vs (ν PO), 1062 vs (ν SiO), 899 w, 892 w, 851 vs (ρ CH₃), 830 m, 771 m, 763 m (ρ CH₃), 683 vs, 619 w, 604 w, 566 w, 545 w. MS (EI 30 eV), m/z (rel int %): 569 (100) [M − CH₃]⁺.

Synthesis of [(Al(hfacac)₂(μ₂-O₂P(OSiMe₃)₂)]₂ (5). To a stirred solution of **1** (0.680 mmol, 407 mg) in toluene (10 mL), excess Hhfacac (0.4 mL, 20 mmol) was added dropwise at 0 °C. The reaction was accompanied by exothermic evolution of gaseous byproducts. The resulting clear colorless solution was then stirred at room temperature for 30 min, and then all volatile components were evaporated under vacuum. Slow cooling of a saturated solution of **5** in hexane to -25 °C provided colorless crystals that were used for X-ray diffraction analysis. Yield: 0.88 g (95%). Mp: subl. 216 °C. ¹H NMR (300.1 MHz, toluene-*d*₈): δ 0.09 (s, C_{2h}, 9H, POSi(CH₃)₃), 0.23 (s, D₂, 36H, POSi(CH₃)₃), 0.34 (s, C_{2h}, 9H, POSi(CH₃)₃), 6.26 (s, 6H, both isomers, (CF₃CO)₂CH). ¹⁹F{¹H} NMR (282.4 MHz, toluene-*d*₈): δ −76.4 (s, 2F, D₂), −76.5 (s, 1F, C_{2h}), −77.6 (s, 2F, D₂), −77.7 (s, 1F, C_{2h}). ²⁷Al NMR (78.1 MHz, toluene-*d*₈): δ −6.0 (s). ²⁹Si{¹H} NMR (99.3 MHz, toluene-*d*₈): 22.6 (s, C_{2h}), 23.8 (s, D₂), 24.2 (s, C_{2h}). ³¹P{¹H} NMR (121.5 MHz, toluene-*d*₈): δ −31.0 (br s, POSi(CH₃)₃). IR (KBr pellet, cm⁻¹): ν 2970 w, 2908 w, 1670 m, 1654 s (ν CO), 1569 m, (ν CO) 1540 m, 1497 m (ν CO + ν CC), 1468 m, 1258 vs (ν CF₃), 1218 s (ν CF₃), 1162 s, 1146 s (δ CH), 1123 m, 1054 m (ν SiO), 854 s (ρ CH₃), 805 m, 764 w (ρ CH₃), 747 w, 671 m, 614 w, 604 w, 593 w, 534 w, 419 w. MS (m/z , rel int): APCI(−) 1364.0098 (100) [M][−] (theor 1364.0116), 1290.9625 (51) [M − SiMe₃][−] (theor 1290.9643). Anal. Calcd for C₃₂H₄₀Al₂F₂₄O₁₆P₂Si₄: C, 28.16; H, 2.95. Found: C, 28.00; H, 2.84. TG/DSC: sublimes at 240–270 °C at atmospheric pressure.

Synthesis of [AlMeAl(hfacac)]₂(μ₃-O₃P(OSiMe₃)₂)]₂(μ₂-O₂P(OSiMe₃)₂)]₂(OP(OSiMe₃)₃) (6). A solution of OP(OH)(OSiMe₃)₂ (1.00 mmol, 242 mg) in toluene (5.0 mL) was added at room temperature to a solution of **1** (0.494 mmol, 295 mg) in toluene (5.0 mL). After evolution of gas ceased, the solution of Hhfacac (0.500 mmol, 104 mg) in toluene (2.0 mL) was added to the reaction mixture. Further evolution of gas was observed. After reaction, all volatile components were removed under vacuum and crystals were grown by slow cooling of the saturated solution of **6** in hexane to -25 °C. Identical product was obtained when the reaction was carried out in THF. Yield: 0.235 g (43% based on Al). Mp: 179–182 °C. ¹H NMR (300.1 MHz, benzene-*d*₆): δ −0.38 (s, 3H, AlCH₃), 0.28 (s, 27H, POSi(CH₃)₃), 0.29 (s, 18H, POSi(CH₃)₃), 0.32 (s, 18H,

POSi(CH₃)₃, 0.52 (s, 18H, POSi(CH₃)₃), 6.23 (s, 1H, (CF₃CO)₂CH), 6.24 (s, 1H, (CF₃CO)₂CH). ¹H NMR (500.1 MHz, dichloromethane-*d*₂): δ -0.99 (s, 3H, AlCH₃), 0.12 (br s, 18H, POSi(CH₃)₃), 0.22 (s, 18H, POSi(CH₃)₃), 0.26 (br s, 18H, POSi(CH₃)₃), 0.30 (s, 27H, POSi(CH₃)₃), 6.01 (s, 1H, (CF₃CO)₂CH), 6.07 (s, 1H, (CF₃CO)₂CH). ¹⁹F{¹H} NMR (282.4 MHz, benzene-*d*₆): δ -75.7 (s, 6F, (CF₃CO)₂CH), -77.0 (s, 6F, (CF₃CO)₂CH). ³¹P{¹H} NMR (121.5 MHz, benzene-*d*₆): δ -23.1 (br s, 2P, μ₃-O₃P(OSiMe₃)), -27.6 (s, 1P, μ₂-O₂P(OSiMe₃)₂), -28.9 (br s, 1P, μ₂-O₂P(OSiMe₃)₂), -32.3 (br s, 1P, OP(OSiMe₃)₃). ³¹P{¹H} NMR (202.4 MHz, dichloromethane-*d*₂): δ -24.7 (br s, 2P, μ₃-O₃P(OSiMe₃)), -29.3 (s, 1P, μ₂-O₂P(OSiMe₃)₂), -30.6 (br s, 1P, μ₂-O₂P(OSiMe₃)₂), -33.9 (br s, 1P, OP(OSiMe₃)₃). ¹³C CP MAS NMR (125.8 MHz): δ -0.86 (AlCH₃), 0.24 (POSi(CH₃)₃), 90.4 (CF₃CO)₂CH, 117.4 (CF₃CO)₂CH, 178.3 (CF₃CO)₂C H). ²⁷Al MAS NMR (130.3 MHz): δ -11.5 (Al^{VI}), -8.7 (Al^{VI}), 46.8 (Al^{IV}). ²⁹Si CP MAS NMR (99.4 MHz): δ 15.8, 16.9, 17.6, 18.6, 20.5, 21.1, 22.3, 25.3 IR (KBr pellet, cm⁻¹): ν 2965 w, 2906 w, 1670 m (νCO), 1559 w (νCO), 1529 m, 1513 m, 1424 w, 1258 vs (νCF₃), 1247 s, 1241 s, 1201 s (νCF₃), 1145 s (δCH), 1117 s (νPO), 1069 s (νSiO), 1046 s, 850 vs (ρCH₃), 795 w, 764 m (ρCH₃), 696 w, 671 w, 613 w, 592 w, 532 w, 489 w. MS (*m/z*, rel int) APCI(+): 1627.1072 (27) [M - Me]⁺ (theor 1627.1140); 1435.1430(63) [M - hfacac]⁺ (theor 1435.1494); 1121.0494 (100) [M - hfacac - OP(OSiMe₃)₃]⁺ (theor 1121.0534). APCI(-): 1535.0356 (58) [M + hfacac - OP(OSiMe₃)₃]⁻ (theor 1535.0301); 1328.0469 (100) [M - OP(OSiMe₃)₃]⁻ (theor 1328.0420). Anal. Calcd for C₃₈H₈₆Al₃F₁₂O₂₄P₅Si₉: C, 27.77; H, 5.27. Found: C, 27.38; H, 5.13.

Synthesis of [Al{Al(hfacac)}₂{μ₃-O₃P(OSiMe₃)₂}{μ₂-O₂P(OSiMe₃)₂}]₂H(OP(O)(OSiMe₃)₂) (7). To a stirred cooled solution (0 °C) of **1** (0.500 mmol, 298 mg) in toluene (5 mL), Hhfacac (0.500 mmol, 104 mg) diluted in toluene (5.0 mL) was added dropwise. The reaction mixture was then warmed to room temperature. After gas evolution ceased, the reaction was cooled down in ice bath and a solution of OP(OH)(OSiMe₃)₂ (1.500 mmol, 373 mg) in toluene (5 mL) was added. The reaction mixture was stirred at 70 °C for 3 h, and then all volatile components were removed under vacuum. Dissolution of an oily residue in a minimum amount of hexane (0.5 mL) with subsequent cooling in a freezer (-25 °C) provided colorless crystals within 2 weeks. Yield: 0.145 g (24% based on Al). Mp: 134–138 °C. ¹H NMR (300.1 MHz, benzene-*d*₆): δ 0.26 (s, 36H, POSi(CH₃)₃), 0.31 (s, 18H, POSi(CH₃)₃), 0.32 (s, 18H, POSi(CH₃)₃), 0.54 (s, 18H, POSi(CH₃)₃), 6.25 (s, 2H, (CF₃CO)₂CH), 14.72 (br s, 1H, POH). ¹⁹F{¹H} NMR (282.4 MHz, benzene-*d*₆): δ -75.9 (s, (CF₃CO)₂CH). ²⁷Al NMR (182.6 MHz, toluene-*d*₈): δ -9.9 (Al^{VI}), 50.3 (Al^{IV}). ³¹P{¹H} NMR (202.4 MHz, toluene-*d*₈): δ -22.7 (s, 1P), -24.8 (s, 2P), -27.7 (br s, 2P), -30.2 (s, 1P). ²⁷Al MAS NMR (182.6 MHz): δ -17.2 (Al^{VI}), -11.9 (Al^{VI}), 47.7 (Al^{IV}). IR (KBr pellet, cm⁻¹): ν 2966 w, 2906 vw, 1672 m (νCO), 1618 vw (νCC), 1560 w (νCO), 1529 w, 1514 w, 1419 vw, 1257 s (νCF₃), 1205 s (νCF₃), 1153 s (δCH), 1147 s (δCH), 1119 m, 1059 s, 850 vs (ρCH₃), 793 w, 762 m (ρCH₃), 696 vw, 671 w, 611 w, 592w, 532w, 501 w. MS (*m/z*, rel int) APCI(-): 1795.1145 (100) (theor 1795.1148) [M - H]⁻, 1761.0554 (78), 1723.0750 (52) [M - SiMe₃]⁻, 1588.1099 (34) [M - hfacac]⁻, 1554.0666 (82) [M - O₂P(OSiMe₃)₂]⁻, 1515.0778 (43) [M - hfacac - SiMe₃]⁻, 1481.0193 (15) [M - O₂P(OSiMe₃)₂ - SiMe₃]⁻.

Synthesis of [(Al(AlMe){Al(hfacac)}₂{μ₃-O₃P(OSiMe₃)₂}{μ₂-O₂P(OSiMe₃)₂}]₂H(OP(O)(OSiMe₃)₂) (8). To a stirred solution of **1** (0.500 mmol, 298 mg) in toluene (5.0 mL) a solution of Hhfacac (1.00 mmol, 208 mg) in toluene (2.0 mL) was added dropwise followed by slow addition of a solution of OP(OH)(OSiMe₃)₂ (1.00 mmol, 242 mg) in toluene (2.0 mL). Both steps were accompanied by evolution of gas. Volatile components were removed under vacuum, and a white solid residue was redissolved in tetrahydrofuran. Cooling below 0 °C provided crystalline product within several days. Yield: 0.120 g (26% based on Al). Mp: 154.5–155.5 °C. ¹H NMR (300.1 MHz, dichloromethane-*d*₂): δ -0.89 (s, 6H, AlCH₃), 0.23, 0.24, 0.26, 0.27, 0.30 (s, 144H, POSi(CH₃)₃), 6.10 (s, 1H, (CF₃CO)₂CH). ¹⁹F{¹H} NMR (282.4 MHz, dichloromethane-*d*₂): δ -76.8 (s, (CF₃CO)₂CH). ³¹P{¹H} NMR (121.5 MHz, dichloromethane-*d*₂): δ -22.8 (br s), -23.8 (s),

-24.6(s), -29.0 (br s). IR (KBr pellet, cm⁻¹): ν 2965 w, 2905 vw, 1670 w (νCO), 1560 w, 1529 w, 1508 w, 1503 w, 1421 vw, 1258 s (νCF₃), 1205 s (νCF₃), 1148 s (δCH), 1119 m, 1053 s (νSiO), 851 vs (ρCH₃), 795 w, 764 w (ρCH₃), 694 w, 671 w, 609 w, 509 w. MS (*m/z*, rel int) APCI(+): 2903.1256 (7) [M - 2Me + hfacac]⁺, 2711.1597 (10) [M - Me]⁺, 2695.1107 (8), 2677.1032 (7), 2639.1199 (5), 2623.0919 (11), 2605.0632 (12), 2485.1384 (40) [M - O₂P(OSiMe₃)₂]⁺, 2413.0953 (17) [M - O₂P(OSiMe₃)₂ - SiMe₃]⁺, 2397.0676 (78) [M - O₂P(OSiMe₃)₂ - SiMe₃ - Me]⁺, 2362.0099 (25) [M - 2O₂P(OSiMe₃)₂ - SiMe₃ - Me + hfacac]⁺, 2324.0298 (17) [M - O₂P(OSiMe₃)₂ - SiMe₃ - OSiMe₃]⁺, 1661.1630 (47) [M/2 + OP(OSiMe₃)₃ - Me]⁺, 1627.1046 (23) [M/2 + SiMe₃ + hfacac - Me]⁺, 1589.1239 (38) [M/2 + OP(OSiMe₃)₂(OH) - Me]⁺, 1435.1400 (100) [M/2 + SiMe₃]⁺, 1363.1007 (40) [M/2 + H]⁺.

Synthesis of [(Al(AlMe){Al(acac)}₂{μ₃-O₃P(OSiMe₃)₂}{μ₂-O₂P(OSiMe₃)₂}]₂H(OP(O)(OSiMe₃)₂) (9). A solution of Hacac (1.00 mmol, 101 mg) in toluene (2 mL) was added dropwise to a solution of **1** (298 mg, 0.500 mmol) in toluene (5 mL) at room temperature. After the evolution of gas ceased, the solution of OP(OH)(OSiMe₃)₂ (1.00 mmol, 242 mg) in toluene (2.0 mL) was transferred dropwise to the reaction mixture and the resulting system stirred at room temperature for 3 h. Volatile components were removed under vacuum, and the solid residue was combined with hexane (4 mL). Formation of crystalline phase was achieved by slow cooling of the saturated solution to -25 °C. Yield: 0.095 g, (23% based on Al). Mp: 138–142 °C. ¹H NMR (300.1 MHz, benzene-*d*₆): δ -0.34 (s, 6H, AlCH₃), 0.26, 0.27, 0.30, 0.41, 0.48 (144H, POSi(CH₃)₃), 1.87 (12H, (CH₃CO)₂CH), 5.28 (2H, (CH₃CO)₂CH). ³¹P{¹H} NMR (121.5 MHz, benzene-*d*₆): δ -21.8 (s, 2P), -23.2 (s, 1P), -28.1 (s, 2P). ¹³C CP MAS NMR (100.55 MHz): δ 1.71 (POSi(CH₃)₃), 27.2 (CH₃CO)₂CH, 188.6 (CH₃CO)₂CH). ²⁷Al MAS NMR (182.6 MHz): δ -15.7 (Al^{VI}), 5.4 (Al^V), 45.1 (Al^{IV}). ²⁹Si CP MAS NMR (79.4 MHz): δ 15.1, 16.9, 17.6, 18.2, 19.7, 20.0, 20.4, 21.1. ³¹P MAS NMR (161.9 MHz): δ -26.9 (2P), -31.4 (2P), -37.9 (1P). IR (KBr pellet, cm⁻¹): ν 2962 w, 2902 vw, 1618 w(νCO), 1535 w, 1460 w, 1414 w, 1255 s (δCH₃), 1207 m, 1144 m, 1115 m, 1045 s (νSiO), 930 vw, 850 vs (ρCH₃), 762 w (ρCH₃), 692 w, 660 vw, 609 w, 579 vw. MS (*m/z*, rel int) ESI(+): 2511.3375 (7) [M + H]⁺ (theor 2511.3360), 2269.2810 (25) [M - O₂P(OSiMe₃)₂]⁺, 2197.2400 (15) [M - O₂P(OSiMe₃)₂ - SiMe₃ + H]⁺, 1954.1831 (13) [M - 2 O₂P(OSiMe₃)₂ - SiMe₃]⁺, 1327.2113 (17) [M/2 + SiMe₃]⁺, 1255.1724 (26) [M/2 + H]⁺, 1013.1155 (100) [M/2 - O₂P(OSiMe₃)₂]⁺.

RESULTS AND DISCUSSION

Reactions of equimolar amounts of OP(OH)(OSiMe₃)₂ with AlR₃ (R = Me, Et, ^tBu) led to elimination of particular alkanes (Scheme 1, Table 1) and provided molecular aluminophosphates **1–3** in good yields. These molecules possess cyclic [Al₂(μ₂-O₂PO₂)₂] cores as shown by the single-crystal X-ray diffraction analyses, mass spectrometry, and NMR spectroscopy measurements. Their synthesis represents a useful extension of known routes for compounds **1** and **2** that were previously prepared by both trimethylsilylchloride and trimethylalkylsilane elimination.²⁴ In contrast to previously published dealkylsilylation condensation of OP(OSiMe₃)₃ with trialkylaluminum compounds, this new approach requires only mild reaction conditions. Moreover, it employs homoleptic aluminum alkyls AlR₃ which unlike AlR₂Cl do not undergo R/Cl ligand scrambling reactions that may complicate product mixtures. Most reactions were accompanied by formation of gaseous byproducts which provided a visible tool for observing the course of the reaction. This synthetic method proved to be particularly useful in producing the new ^tBu derivative **3** because bulkier organic groups on the Al atoms hinder dealkylsilylation of OP(OSiMe₃)₃ with Al^tBu₃ and the adduct Al^tBu₃-OP(OSiMe₃)₃ showed only a low conversion to cyclic aluminophosphate **3**. An extension of our dealkylsilylation

principle to the reaction of ${}^c\text{HexP}(\text{O})(\text{OSiMe}_3)_2$ with AlMe_3 showed its applicability to the synthesis of aluminophosphonates. Unsymmetrically substituted cyclic $[(\text{AlMe}_2\{\mu_2\text{-O}_2\text{P}(\text{OSiMe}_3)({}^c\text{Hex})\})_2]$ (*cis/trans*-4, Chart 2S, Supporting Information) was prepared by Me_4Si elimination, and its *trans* isomer was structurally characterized. The molecular structure of *trans*-4 is presented in Figure 1, and the bonding metrics are

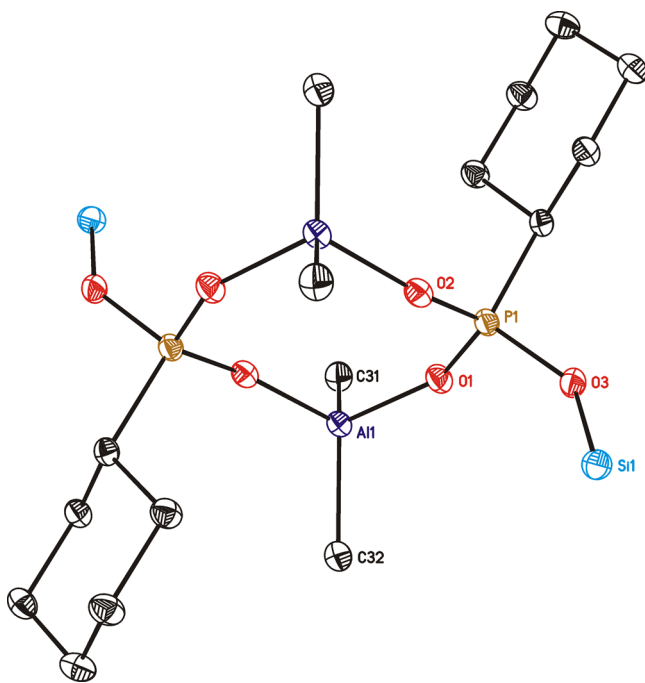


Figure 1. Molecular structure of *trans*-4. All CH_3 groups at Si and H atoms of ${}^c\text{Hex}$ and $\text{Al}-\text{CH}_3$ substituents were omitted for clarity. Thermal ellipsoids are drawn at the 30% probability level.

gathered in Table 3. Bond distances and angles compare well with the corresponding parameters in the related molecule $\mathbf{12}^{25}$ and other cyclic $[\text{Al}_2(\mu_2\text{-O}_2\text{PO}_2)_2]$ cores.

${}^1\text{H}$ NMR spectra of **4** revealed the presence of both isomers. Molecular symmetry of the *cis* isomer (C_{2v}) resulted in two resonances of the $\text{Al}(\text{CH}_3)_2$ moieties at -1.18 and -1.15 ppm, while the *trans* isomer (C_{2h}) revealed only one at -1.16 ppm. The resonances of $\text{POSi}(\text{CH}_3)_3$ were not resolved in two separate lines. Even though the ${}^{13}\text{C}\{{}^1\text{H}\}$ NMR spectra displayed only one broad resonance for $\text{Al}(\text{CH}_3)_2$ at -9.57 ppm, the presence of two isomers was revealed in two doublets of $\text{POSi}(\text{CH}_3)_3$ groups at 1.07 and 1.12 ppm and two doublets for the tertiary carbons of the ${}^c\text{Hex}$ substituents at 36.63 and 36.67 ppm. Similarly, ${}^{31}\text{P}\{{}^1\text{H}\}$ NMR spectra show two expected singlet resonances at 12.7 (*cis*) and 13.0 (*trans*) ppm of integral intensities of 0.8:1; presumed higher thermodynamic stability of the *trans* configuration prompted us to assign to it the latter signal.²⁵ The ${}^{29}\text{Si}\{{}^1\text{H}\}$ NMR spectrum also revealed two different resonances at 22.4 and 22.6 ppm for *cis* and *trans*, respectively. The stability of the cyclic $[\text{Al}_2(\mu_2\text{-O}_2\text{PO}_2)_2]$ core in the gas phase was exhibited in the EI mass spectrum by the base peak at m/z 569 for the $[\text{M} - \text{CH}_3]^+$ fragment.

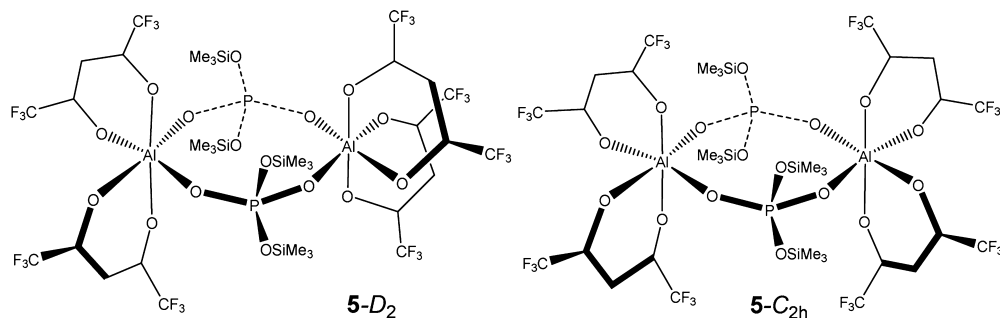
For our further studies of reactivity of the aluminophosphate S4R molecules, we selected compound **1** as a starting point. This simplest building unit can be used for structural description and computer modeling of many types of zeolitic frameworks.⁴⁶ Interestingly, molecular four rings were identi-

Table 3. Comparison of Selected Bond Distances (Angstroms) and Angles (degrees)^a in S4R Type of Aluminophosphates **1**, **2**,^b **10**, **11**, **13**, and **(14)**₂ and Aluminophosphonates **4**, **12**, and $[(\text{R}_2\text{Al}(\mu_2\text{-O})_2\text{PZY})_2]$, see Scheme 1 and Table 1

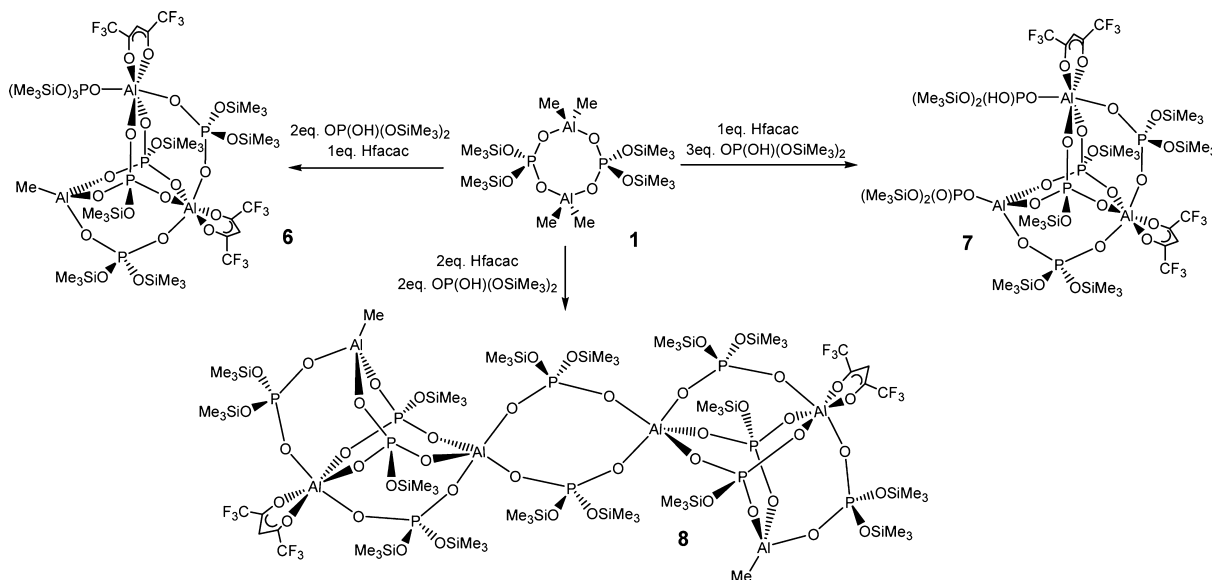
	1 ²⁴	2A ²⁴	2B ²⁴	10 ²²	11 ²³	13 ²⁶	14 ²³	4	12 ²⁵
P–O intraring	1.503(3)	1.445(4)	1.463(5)	1.470(6)	1.442(4)	1.488(5)	1.465(6)–1.496(5)	1.512(3)	1.508(4)
P–O extraring	1.541(3)	1.486(4)	1.491(5)	1.504(6)	1.463(4)	1.572(2)	1.492(7)–1.539(7)	1.557(2)	1.533(3)
Al–O	1.811(3)	1.496(6)	1.508(6)	1.798(6)	1.490(7)	1.816(2)	1.754(5)–1.896(5)	1.801(2)	1.787(3)
Al–C	1.954(4)	1.98(2)	1.98(2)	1.972(7)	1.785(4)	1.975(2)–1.990(2)	1.964(4)	1.956(7)	1.813(3)
Si–O	1.672(3)	1.641(6)	1.627(5)	1.650(4)	1.933(10)	1.682(2)	1.688(3)	1.669(5)	1.628(4)
Al–O–P	148.0(1)	159.1(3)	150.0(4)	160.9(3)	156.7(4)	150.33(8)–156.12(8)	149.6(4)–159.9(5)	150.4(1)	144.9(2)
O–P–O intraring	146.5(1)	152.4(3)	147.1(3)	151.4(2)	113.9(3)	117.48(7), 117.79(7)	115.4(4)	163.7(1)	158.2(2)
O–Al–O	114.7(1)	114.8(3)	115.0(3)	113.6(2)	102.8(2)	101.75(6), 100.15(6)	105.1(3), 89.3(2)	113.1(1)	113.5(2)
	101.3(1)	103.2(2)	102.1(2)	102.3(2)	102.8(2)			103.1(1)	100.5(2)

^aPairs of independent parameters within the molecules were averaged when their difference (Δ) was smaller than $3\sigma\Delta$. ^bTwo independent half-molecules, **2A** and **2B**.

Chart 1. Two Isomeric Forms of Cyclic Aluminophosphate 5



Scheme 2. Reactions Leading to Molecular Aluminophosphates 6, 7, and 8



fied by NMR spectroscopic methods in hydrothermal reaction solutions during the course of aluminophosphate crystallization.^{47,48} The precursor **1** possesses reactive functionalities both on Al and on P atoms and could be used for building larger units. We selected two reagents; $\text{OP(OH)(OSiMe}_3)_2$ was expected to react preferentially with the Al–CH₃ groups, by either CH₄ or Me₄Si elimination, extend the molecule, and change the Al/P ratio. The second reagent was chelating pentanedione as a capping agent that would saturate the coordination sphere of Al and prevent uncontrolled oligo/polymerization of these polyfunctional reagents and formation of untractable mixtures. Hhfacc was chosen over Hfacac, which reacts with **1** to completely dismember its cyclic molecule to Al(acac)_3 . Interestingly, Hfacac was shown to promote cage rearrangement of a cubic aluminophosphonate [$\{^t\text{BuAl}(\mu_3\text{-O}_3\text{PMe})\}_4$] to decameric [$\{^t\text{BuAl}(\mu_3\text{-O}_3\text{PMe})\}_{10}$] without being incorporated in the product.²⁸

The combination **1** with excess Hhfacc led to gas evolution, which suggested replacement of methyl groups originally bonded to the Al atoms by hfacac ligands accompanied by CH₄ release. The reaction proceeded quantitatively according to NMR measurements, no byproducts were observed, and a crystalline product was obtained. X-ray diffraction analysis revealed molecular structures of **5** belonging to the D_2 point group (Chart 1).⁴⁹ The inorganic $[\text{Al}_2(\mu_2\text{-O}_2\text{PO}_2)_2]$ core of the starting aluminophosphate is retained; however, both Al atoms in **5** are chelated by two hfacac ligands and display octahedral

coordination environments. Multinuclear NMR study of the reaction mixture reveals two sets of signals representing two isomeric forms of **5**. The isomerism arises from two different orientations of the hfacac substituents (Chart 1). The integral intensity of representative signals in the NMR spectra suggests a 1:2 ratio of C_{2h} and D_2 forms. Compound **5** was surprisingly stable against hydrolysis. No changes were observed after 24 h treatment with H₂O at room temperature. The ³¹P NMR spectrum of **5** at room temperature contained only one broad resonance at –31.0 ppm, but after cooling to –20 °C the signal shifted downfield and split to two resonances (–30.1 and –30.4 ppm, approximately 2:1) representing the two isomers of **5**. The ¹H NMR spectrum contained three signals of Me₃Si groups; their integral intensities were in the 1:4:1 ratio and thus agreed with the 1:2 molar ratio of isomers (C_{2h} : D_2). Methine hydrogens showed only one resonance at room temperature, which was split in two signals at –20 °C. The dynamic nature of the C_{2h} / D_2 isomer equilibrium was revealed in the ¹⁹F NMR spectra. Four singlets of the CF₃ groups were observed at room temperature, while at 90 °C, the two low-field singlets coalesced and the two high-field ones started to overlap.

Reaction of cyclic **1** with 2 equiv of $\text{OP(OH)(OSiMe}_3)_2$ followed by addition of 1 equiv of Hhfacc (Scheme 2) provided a new aluminophosphate cluster **6**. Single-crystal X-ray diffraction analysis revealed the molecule to contain three Al and five P atoms (Figure 2). One aluminum atom is four coordinate with one unreacted CH₃ group, while the other two

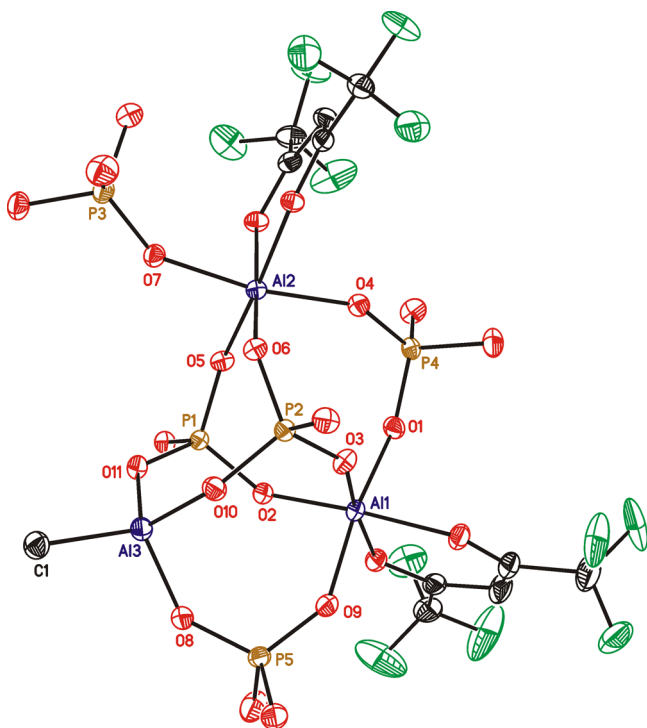


Figure 2. Molecular structure of **6**. All SiMe_3 and H atoms at CH_3 and hfacac groups were omitted for clarity. Thermal ellipsoids are drawn at the 30% probability level.

Al are six coordinate with capping hfacac ligands. The Al centers are connected by two tridentate $[\mu_3\text{-O}_3\text{P}(\text{OSiMe}_3)]^{2-}$ and two bidentate $[\mu_2\text{-O}_2\text{P}(\text{OSiMe}_3)_2]^-$ bridging phosphates. One of the octahedral Al atoms is coordinated by the phosphoryl oxygen of $\text{OP}(\text{OSiMe}_3)_3$. This points to a silylation of the starting diester $\text{OP}(\text{OH})(\text{OSiMe}_3)_2$ during the reaction. One can identify the 4=1 zeolitic SBU (Chart 2) in the framework of **6**. This unit, however, is extended by two $[\mu_2\text{-O}_2\text{P}(\text{OSiMe}_3)_2]^-$ bridges and a terminal $\text{OP}(\text{OSiMe}_3)_3$ group. A related aluminophosphate cage **15** was structurally characterized, possesses all Al atoms in octahedral coordination environment, and also contains two extra AlCl_3 molecules coordinated at the periphery (Chart 2).⁵⁰

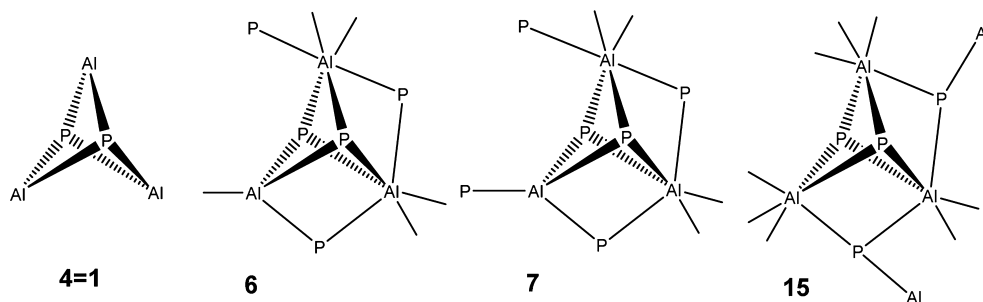
The bonding distances reveal elongation of the Al–O(P) bonds with increasing coordination number of Al. Tetrahedral Al3–O(P) bonds fall into a narrow range 1.770(2)–1.777(2) Å (average 1.774 Å), which corresponds well with the values found in corner $\text{CH}_3\text{-AlO}_3$ groups (average 1.76 Å) of tetrameric cubic aluminophosphate $[\{\text{MeAl}(\mu_3\text{-O}_3\text{PPh})\}_4]$.⁵¹ Octahedral Al–O(P) bonds are longer (1.818(2)–1.891(2) Å),

and the longest Al–O(P) distance in complex **6** is the coordination bond to $\text{OP}(\text{OSiMe}_3)_3$ (Al2–O7 1.891(2) Å). Interestingly, the P3–O7 bond in this moiety is at the shortest end of the P–O(Al) range (1.469(2)–1.532(2) Å). The P–O(Al) bonds involving tetrahedral Al atoms and tridentate $[\mu_3\text{-O}_3\text{P}(\text{OSiMe}_3)]^{2-}$ are longer (1.53 Å) in comparison with octahedral (1.50 Å). Al–O–P bond angles are from 130.1(2)° to 146.5(1)°.

^1H , $^{19}\text{F}\{^1\text{H}\}$, and $^{31}\text{P}\{^1\text{H}\}$ NMR spectra correspond with the C_s molecular symmetry of **6** in solution. The methyl group on aluminum presents a high-field singlet in the ^1H NMR at -0.38 ppm. The resonances at 0.28, 0.29, 0.32, and 0.52 ppm in a 3:2:2:2 intensity ratio represent the inequivalent trimethylsilyl groups. The pair of singlet resonances at 6.23 and 6.24 belongs to methine hydrogens of two distinct hfacac ligands. Their CF_3 resonances in the $^{19}\text{F}\{^1\text{H}\}$ spectrum at -75.69 and -76.98 ppm are in the expected 1:1 ratio. The $^{31}\text{P}\{^1\text{H}\}$ NMR spectrum displays four broadened resonances at -23.1 , -27.6 , -28.9 , and -32.3 in a 2:1:1:1 ratio that may be assigned to $[\mu_3\text{-O}_3\text{P}(\text{OSiMe}_3)]^{2-}$, $[\mu_2\text{-O}_2\text{P}(\text{OSiMe}_3)_2]^-$, $[\mu_2\text{-O}_2\text{P}(\text{OSiMe}_3)_2]^-$, and $\text{OP}(\text{OSiMe}_3)_3$ moieties, respectively. The most shielded signal represents tris(trimethylsilyl)ester coordinated to one Al atom. Broadening of signals points to a dynamic chemical exchange process. Low-temperature ^1H and $^{31}\text{P}\{^1\text{H}\}$ NMR spectra were acquired in the range from $+30$ to -80 °C. The width of signals decreased on cooling; however, the number of signals remained unchanged. Solid-state ^{13}C CP MAS NMR spectra revealed only one set of resonances for the hfacac ligands (178.3, 117.4, and 90.4 ppm) and two signals (0.24 and -0.86 ppm) for unresolved trimethylsilyl groups. The ^{27}Al MAS NMR spectrum featured four-coordinate Al at 46.8 ppm and octahedral Al atoms at -8.7 and -11.5 ppm. Eight resolved resonances in the ^{29}Si CP MAS NMR spectrum is in accord with 9 trimethylsilyl groups in **6** considering a general position of the molecule in the unit cell. The mass spectra $\text{APCI}(\pm)$ demonstrate the stability of the $\text{Al}_3(\text{PO}_4)_4$ inorganic core.

Changing the order of reagent addition and using one extra equivalent of $\text{OP}(\text{OH})(\text{OSiMe}_3)_2$ (Scheme 2) we isolated **7** that is closely related to **6** in having the same inorganic core. However, **7** differs from **6** in substitution of the CH_3 group at tetrahedral Al by the $-\text{OP}(\text{O})(\text{OSiMe}_3)_2$ moiety and one molecule of $\text{OP}(\text{OH})(\text{OSiMe}_3)_2$ instead of $\text{OP}(\text{OSiMe}_3)_3$ being coordinated to the octahedral Al atom. The molecular structure of **7** is shown in Figure 3 and features a C_s molecular symmetry. The Al–O(P) bonds at the tetrahedral Al atom are in the range Al(3A) 1.729(4)–1.757(3) Å, while at the octahedral Al atoms are longer 1.823(3)–1.888(3) Å. Similarly to **6**, one can distinguish longer P–O(Al) bonds directed toward tetrahedral Al atoms in comparison to the bonds with

Chart 2. Molecules Containing the Structural Motif of a 4=1 Secondary Building Unit



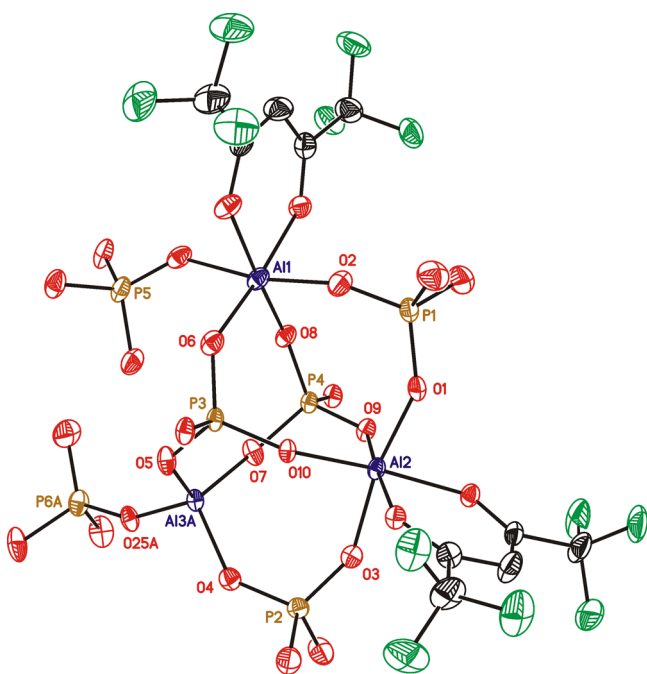
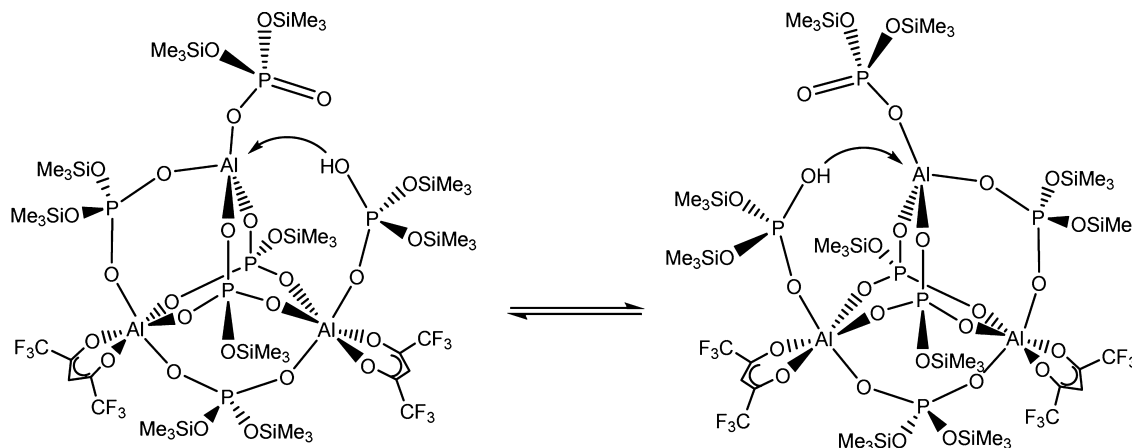


Figure 3. Molecular structure of **7**. All SiMe_3 groups and H atoms of hfacac and $\text{OP}(\text{OH})(\text{OSiMe}_3)_2$ ligands were omitted for clarity. Thermal ellipsoids are drawn at the 30% probability level.

six-coordinate Al atoms. The Al–O–P bond angles in the molecule **7** are found in a broader range ($115.6(4)$ – $162.3(2)^\circ$) than in **6**.

Disorder in the crystal structure of **7** at $\text{O}_2\text{P}(\text{OSiMe}_3)_2$ groups connected to a four-coordinate Al atom together with the results of the NMR spectroscopy showing a higher molecular symmetry C_{2v} than expected from X-ray structural analysis suggest a dynamic tautomeric exchange in solution (Scheme 3). Although the P–OH proton was not located in the electron density map, a low-field resonance at 14.72 ppm may be assigned to it in the ^1H NMR spectrum. It contains only 4 resonances of the trimethylsilyl groups (0.26, 0.31, 0.32, and 0.54 ppm) in a 2:1:1:1 ratio, and also the methines of the hfacac groups display only one singlet at 6.25 ppm. Similarly, only one resonance in the $^{19}\text{F}\{^1\text{H}\}$ NMR spectrum suggests chemical equivalence of the hfacac groups. The ^{27}Al NMR spectrum reveals only one signal of the octahedral Al atoms at

Scheme 3. Possible Dynamic Exchange Process in **7**



–9.9 ppm and one at 50.3 ppm representing the unique Al center. Four broad signals in the $^{31}\text{P}\{^1\text{H}\}$ NMR spectrum at –22.7, –24.8, –27.7, and –30.2 ppm in a 1:2:2:1 intensity ratio also suggest an intramolecular dynamic process. The solid-state ^{27}Al MAS NMR spectrum represents the static structure of **7** with three inequivalent Al atoms, two octahedral at –17.2 and –11.9 ppm and one four-coordinate at 47.7 ppm. Mass spectra display as the base peak the molecular fragment $[\text{M} - \text{H}]^-$ at m/z 1795 attesting to a good stability of the cluster framework.

Using a relatively large proportion of the capping Hhfacac reagent in comparison to $\text{OP}(\text{OH})(\text{OSiMe}_3)_2$ (Scheme 2), we isolated the hexanuclear cluster **8**. Single-crystal X-ray diffraction analysis revealed the molecular structure depicted in Figure 4. This aluminophosphate contains Al and P atoms in

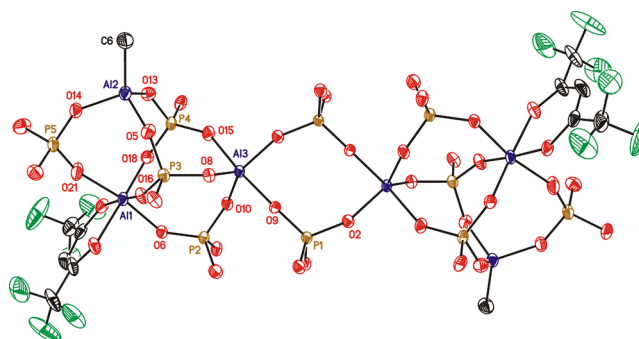
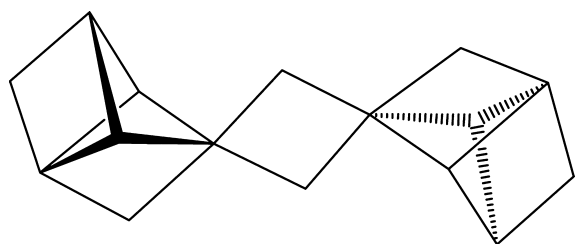


Figure 4. Molecular structures of **8**. All SiMe_3 groups and H atoms of Al– CH_3 and hfacac ligands were omitted for clarity. Thermal ellipsoids are drawn at the 30% probability level.

a 3:5 ratio. The centrosymmetric molecule (point group C_i) is constructed from one four ring of the starting molecule **1** and two 4=1 units analogous to **6** and **7** (Charts 2 and 3). The Al atoms of the central four ring are shared with the peripheral units making them five coordinate. That contributes to the presence of Al centers in three different coordination environments: 4, 5, and 6. There are two types of phosphate bridging units: four tridentate $[\mu_3\text{-O}_3\text{P}(\text{OSiMe}_3)]^{2-}$ and six bidentate $[\mu_2\text{-O}_2\text{P}(\text{OSiMe}_3)_2]^-$.

Al–O(P) bond distances correspond to a particular coordination number of the Al atoms and fall in the following ranges: Al(CN 4) 1.754(3)–1.772(3) Å, Al(CN 5) 1.789(3)–1.864(3) Å, and Al(CN 6) 1.829(3)–1.877(3) Å. The P–

Chart 3. Schematic Representation of Molecule of 8 Emphasizing the 4=1 and S4R Structural Motifs



O(Al) bonds are in the 1.460(3)–1.5439(3) Å range. The coordination geometry around Al centers is thus described as deformed tetrahedral (CN 4), trigonal bipyramidal (CN 5, $\beta = 174.89^\circ$, $\alpha = 123.29^\circ$, $\tau = 86\%$),⁵² and deformed octahedral (CN 6). Al–O–P bond angles are 134.7(2)–160.8(2)°.

The ¹H NMR spectrum displays a singlet at –0.89 ppm for the methyl group on a four-coordinate Al atom. Five singlet resonances at 0.23–0.30 ppm represent trimethylsilyl groups, and one at 6.13 ppm belongs to hfacac methines. The ¹⁹F{¹H} spectrum displays only one singlet at –76.8 ppm for the CF₃ groups. This suggests a conformational fluxional process at the five-coordinate Al centers as there is no plane of symmetry in the molecule in the solid state (point group C_i) (Figure 4). The ³¹P{¹H} NMR spectrum features only four signals at –22.8, –23.8, –24.6 (sharp), –29.0 ppm that represent symmetry inequivalent P atoms of the phosphate groups, pointing again to a fluxional process introducing mirror symmetry.

Replacing Hhfacac by Hacac as the capping agent, we prepared and structurally characterized **9** that is isostructural with **8**. The molecular structure of **9** is shown in Figure 1S, Supporting Information. Al–O(P) bond distances are Al(CN 4) 1.752(4)–1.81(3) Å, Al(CN 5) 1.780(3)–1.870(4) Å, and Al(CN 6) 1.826(4)–1.904(8) Å. P–O(Al) bonds fall in the range 1.465(8)–1.528(4) Å. The environment of the Al atom in the trigonal bipyramidal site is slightly deformed ($\beta = 175.41^\circ$, $\alpha = 123.46^\circ$, $\tau = 87\%$ ⁵²). Al–O–P bond angles are 133.9(3)–159.4(2)°.

CONCLUSIONS

Reactions of equimolar OP(OH)(OSiMe₃)₂ and trialkylalanes provide molecular cyclic compounds [(AlR₂{μ₂-O₂P(OSiMe₃)₂})₂], R = Me (**1**), Et (**2**), ⁱBu (**3**), by alkane elimination, while unsymmetrically substituted [(AlMe₂{μ₂-O₂P(OSiMe₃)₂(^cHex)})₂] (*cis/trans*-**4**) is prepared by dealkylsilylation reaction of ^cHexP(O)(OSiMe₃)₂ with AlMe₃. These molecules present cyclic [Al₂(μ₂-O₂PO₂)₂] aluminophosphate cores that mimic the single four-ring building unit (S4R) of zeolitic, layered, and chain aluminophosphates. The findings represent a useful extension of known methods leading to molecular aluminophosphates as it allows preparation of cyclic aluminophosphates bearing bulkier organic groups on Al atoms. The presence of reactive methyl groups bonded to Al atoms motivated us to further study the reactivity of a selected representative of this family of building units. Compound **1** was used in reactions with Hhfacac, used as a capping agent to control growth of aluminophosphate molecules by saturating Al coordination sites, and with OP(OH)(OSiMe₃)₂, employed as a bridging reagent, with the aim to extend this simplest four ring to larger cage aluminophosphates. We successfully prepared and structurally characterized a series of five new molecular aluminophosphates **5–9** of different nuclearity.

Reaction of **1** with excess Hhfacac results in replacement of all four methyl groups by chelating hfacac ligands, and the obtained molecular compound **5** contains two octahedrally coordinated Al atoms. The molecules of **5** display geometric isomerism caused by two possible mutual positions of hfacac substituents. The presence of both C_{2h} and D₂ forms in the reaction mixture was evidenced by NMR spectroscopy. Further linking of cyclic molecule **1** to higher aluminophosphates by excess OP(OH)(OSiMe₃)₂ leads to cage molecules **6** and **7**. They contain in their inorganic core the [Al₃{μ₃-O₃P(OSiMe₃)₂}₂{μ₂-O₂P(OSiMe₃)₂}₂] units that can be thought of as the 4=1 building units of zeolites with two extra phosphate bridges. Finally, tuning the reagent ratio lead to formation of large cluster [(Al(AlMe){Al(hfacac)}{μ₃-O₃P(OSiMe₃)₂}₂{μ₂-O₂P(OSiMe₃)₂}₃})₂] **8** containing the central S4R ring with two peripheral 4=1 structural units attached. Isostructural compound **9** is isolated when Hacac is used instead of Hhfacac. Both molecules display the Al centers in four-, five-, and six-coordinate environments. The isolated series of aluminophosphate molecules demonstrates the ability to build larger structural units by a controlled step-by-step process employing a simple molecular four-ring (S4R) precursor **1**, OP(OH)(OSiMe₃)₂ as a phosphate source, and Hhfacac as a capping reagent. The single four ring is first extended to a bridged four ring (4=1) and then to a complex structure containing a larger assembly of the building blocks.

ASSOCIATED CONTENT

Supporting Information

Complete X-ray data for compounds **4–9**. This material is available free of charge via the Internet at <http://pubs.acs.org>.

AUTHOR INFORMATION

Corresponding Author

*Phone: +420549496493. Fax: +420549492443. E-mail: jpinkas@chemi.muni.cz.

Notes

The authors declare no competing financial interest.

ACKNOWLEDGMENTS

This work was supported by CEITEC (Central European Institute of Technology (CZ.1.05/1.1.00/02.0068)), by the project Employment of Best Young Scientists for International Cooperation Empowerment (CZ.1.07/2.3.00/30.0037), and by MOBILITY 7AMB13DE006. The authors thank Dr. Z. Zdrahal and B. Vrbkova (MU) for MS measurements, Dr. C. E. Barnes and Dr. J. Abbott for solid-state NMR (University of Tennessee), and Dr. V. Jancik (UNAM) for CHN analyses.

DEDICATION

Dedicated to Professor J. G. Verkade on the occasion of his 79th birthday.

REFERENCES

- Cheetham, A. K.; Ferey, G.; Loiseau, T. *Angew. Chem., Int. Ed.* **1999**, *38*, 3268–3292.
- Harrison, W. T. A. *Curr. Opin. Solid State Mater. Sci.* **2002**, *6*, 407–413.
- Feng, S.; Xu, R. *Acc. Chem. Res.* **2001**, *34*, 239–247.
- Morris, R. E.; Weigel, S. J. *Chem. Soc. Rev.* **1997**, *26*, 309–317.
- Parnham, E. R.; Morris, R. E. *Acc. Chem. Res.* **2007**, *40*, 1005–1013.

- (6) Martinez, C.; Corma, A. *Coord. Chem. Rev.* **2011**, *255*, 1558–1580.
- (7) Weckhuysen, B. M.; Rao, R. R.; Martens, J. A.; Schoonheydt, R. A. *Eur. J. Inorg. Chem.* **1999**, *4*, 565–577.
- (8) Thomas, J. M.; Hernandez-Garrido, J. C.; Raja, R.; Bell, R. G. *Phys. Chem. Chem. Phys.* **2009**, *11*, 2799–2825.
- (9) Rajic, N. *J. Serb. Chem. Soc.* **2005**, *70*, 371–391.
- (10) Yu, J.; Xu, R. *Acc. Chem. Res.* **2010**, *43*, 1195–1204.
- (11) Yu, J.; Xu, R.; Li, J. *Solid State Sci.* **2000**, *2*, 181–192.
- (12) Yu, J.; Xu, R. *Acc. Chem. Res.* **2003**, *36*, 481–490.
- (13) Yu, J.; Xu, R. *Chem. Soc. Rev.* **2006**, *35*, 593–604.
- (14) Férey, G. *Chem. Mater.* **2001**, *13*, 3084–3098.
- (15) Férey, G. *J. Fluorine Chem.* **1995**, *72*, 187–193.
- (16) Taulelle, F. *Solid State Sci.* **2001**, *3*, 795–800.
- (17) Oliver, S.; Kuperman, A.; Ozin, G. A. *Angew. Chem., Int. Ed.* **1998**, *37*, 46–62.
- (18) Rao, C. N. R.; Natarajan, S.; Choudhury, A.; Neeraj, S.; Ayi, A. A. *Acc. Chem. Res.* **2001**, *34*, 80–87.
- (19) Murugavel, R.; Choudhury, A.; Walawalkar, M. G.; Pothiraja, R.; Rao, C. N. R. *Chem. Rev.* **2008**, *108*, 3549–3655.
- (20) Mason, M. R. *J. Cluster Sci.* **1998**, *9*, 1–23.
- (21) Walawalkar, M. G.; Roesky, H. W.; Murugavel, R. *Acc. Chem. Res.* **1999**, *32*, 117–126.
- (22) Mason, M. R.; Matthews, R. M.; Mashuta, M. S.; Richardson, J. F. *Inorg. Chem.* **1996**, *35*, 5756–5757.
- (23) Lugmair, C. G.; Tilley, T. D.; Rheingold, A. L. *Chem. Mater.* **1999**, *11*, 1615–1620.
- (24) Pinkas, J.; Chakraborty, D.; Yang, Y.; Murugavel, R.; Noltemeyer, M.; Roesky, H. W. *Organometallics* **1999**, *18*, 523–528.
- (25) Chakraborty, D.; Horchler, S.; Kraetzner, R.; Varkey, S. P.; Pinkas, J.; Roesky, H. W.; Uson, I.; Noltemeyer, M.; Schmidt, H.-G. *Inorg. Chem.* **2001**, *40*, 2620–2624.
- (26) Florjanczyk, Z.; Lasota, A.; Wolak, A.; Zachara, J. *Chem. Mater.* **2006**, *18*, 1995–2003.
- (27) Furdala, K. L.; Tilley, T. D. *J. Am. Chem. Soc.* **2001**, *123*, 10133–10134.
- (28) Mason, M. R.; Perkins, A. M.; Ponomarova, V. V.; Vij, A. *Organometallics* **2001**, *20*, 4833–4839.
- (29) Cassidy, J. E.; Jarvis, J. A. J.; Rothon, R. N. *J. Chem. Soc., Dalton Trans.* **1975**, 1497–1499.
- (30) Yang, Y.; Schmidt, H.-G.; Noltemeyer, M.; Pinkas, J.; Roesky, H. W. *J. Chem. Soc., Dalton Trans.* **1996**, 3609–3610.
- (31) Azais, T.; Bonhomme, Ch.; Bonhomme-Courty, L.; Vaisermann, J.; Millot, Y.; Man, P. P.; Bertani, P.; Hirschinger, J.; Livage, J. *J. Chem. Soc., Dalton Trans.* **2002**, 609–618.
- (32) Mason, M. R.; Matthews, R. M.; Perkins, A. M.; Ponomarova, V. V. *ACS Symp. Ser.* **2002**, *822*, 181–194.
- (33) Yang, Y.; Walawalkar, M. G.; Pinkas, J.; Roesky, H. W.; Schmidt, H.-G. *Angew. Chem., Int. Ed. Engl.* **1998**, *37*, 96–98.
- (34) Yang, Y.; Pinkas, J.; Noltemeyer, M.; Roesky, H. W. *Inorg. Chem.* **1998**, *37*, 6404–6405.
- (35) Yang, Y.; Pinkas, J.; Schaefer, M.; Roesky, H. W. *Angew. Chem., Int. Ed. Engl.* **1998**, *37*, 2650–2653.
- (36) Azais, T.; Bonhomme-Courty, L.; Vaisermann, J.; Maquet, J.; Bonhomme, C. *Eur. J. Inorg. Chem.* **2002**, 2838–2843.
- (37) Azais, T.; Bonhomme, C.; Bonhomme-Courty, L.; Kickelbick, G. *Dalton Trans.* **2003**, 3158–3159.
- (38) Murugavel, R.; Kuppuswamy, S. *Angew. Chem., Int. Ed.* **2006**, *45*, 7022–7026.
- (39) Wulff-Molder, D.; Meisel, M. *Z. Kristallogr.* **1998**, *213*, 353–355.
- (40) Murugavel, R.; Kuppuswamy, S. *Chem.—Eur. J.* **2008**, *14*, 3869–3873.
- (41) Murugavel, R.; Gogoi, N. *J. Organomet. Chem.* **2010**, *695*, 916–924.
- (42) Pinkas, J.; Wessel, H.; Yang, Y.; Montero, M. L.; Noltemeyer, M.; Fröba, M.; Roesky, H. W. *Inorg. Chem.* **1998**, *37*, 2450–2457.
- (43) Pinkas, J.; Löbl, J.; Dastyk, D.; Necas, M.; Roesky, H. W. *Inorg. Chem.* **2002**, *41*, 6914–6918.
- (44) Andrianov, K. A.; Rutovskii, B. N.; Kazakova, A. A. *Zh. Obshch. Khim.* **1956**, *26*, 267 (engl. Ausg. S.285).
- (45) Sheldrick, G. M. *Acta Crystallogr., Sect. A* **2008**, *64*, 112–122.
- (46) Peskov, M. V.; Blatov, V. A.; Ilyushin, G. D.; Schwingschlögl, U. *J. Phys. Chem. C* **2012**, *116*, 6734–6744.
- (47) Vistad, Ø. B.; Akporiaye, D. E.; Taulelle, F.; Lillerud, K. P. *Chem. Mater.* **2003**, *15*, 1639–1649.
- (48) Férey, G.; Haouas, M.; Loiseau, T.; Taulelle, F. *Chem. Mater.* **2014**, *26*, 299–309.
- (49) Crystals of **5** were orthorhombic (space group $P2_12_12$), with lattice parameters $a = 13.606(2)$ Å, $b = 17.948(4)$ Å, $c = 11.7686(15)$ Å, $V = 2873.9(9)$ Å³. Because of poor crystal quality and low diffraction intensity at high resolution, the structure was solved and refined using a data set cut at $\sin \theta/\lambda = 0.48$ Å⁻¹. Flack test results were ambiguous; therefore, Friedel pairs were merged, giving a data to parameter ratio of ca. 4.3. Refinement converged at an R value of 0.1082 ($I > 2\sigma(I)$). The esd's of derived bond lengths and angles were larger (by an order of magnitude) than those for other present structures and thus excluded from comparison.
- (50) Richards, A. F.; Beavers, C. M. *Dalton Trans.* **2012**, *41*, 11305–11310.
- (51) Yang, Y. Dissertation, University of Goettingen, Germany, 1999.
- (52) Addison, A. W.; Rao, T. N.; Reedijk, J.; Rijn, J.; van Verschoor, G. C. *J. Chem. Soc., Dalton Trans.* **1984**, 1349–1356.